Diurnal Change of Wall Flows and Energy Balance on the South Facing Wall When Background Wind is Absent

Yifan Fan[1,*], Yuguo Li[1], Jian Hang[2] and Kai Wang[1]

[1]Department of Mechanical Engineering, the University of Hong Kong, Hong Kong
[2]Department of Atmospheric Sciences, School of Environmental Science and Engineering, Sun Yat-Sen University, Guangzhou, China
*corresponding author: u3002019@hku.hk

Abstract The in-situ measurement of wall flows during clear days on a 16 story building in Guangzhou, China is introduced and analyzed in this paper. The surface temperature was measured by infrared camera and thermal couples. The ambient temperature, relative humidity, wind velocity and solar radiation were recorded by weather stations. The Rayleigh number of wall flows reached as high as 1.44×10^{14}.
We found that the different kind of heat flux reach its maximum value in a day cycle at different time. The transmittance of the atmosphere keeps decreasing from the sunrise to the sunset in Guangzhou typical clear days. The wall surface temperature and flow were visualized by Infrared videos. The diurnal change of energy balance on the south facing wall was calculated based on the solar radiation, long wave radiation and heat transfer caused by natural convection adjacent to the wall.
Keywords: Wall flows, Energy balance

1. Introduction

The wall flow is important in ventilating a city and building energy balance when there is no synoptic wind [1] [2] [3] [4] [5] [6] [7] [8]. Even the background wind exists, it would be blocked by the dense high-rise buildings in the urban area [9] [10] [11] [12].The energy balance in the building walls can influence both indoor and outdoor environment in thermal comfort, energy saving and urban ventilation. Natural convective heat transfer is a connection between the flow in the urban canopy layer and the energy balance in building walls. To study the energy balance in the urban canopy layer, the mechanism of the wall flows caused by natural convection must be also well understood.
Natural convection along a vertical heated plate (wall flows) has been studied for a long time [13] [14] [15] [16] [17], while the flow and heat transfer along a real high-rise building wall caused by natural convection was never measured due to the difficulty in finding a high-rise building with a flat wall, getting the permission of taking measurement and installing the measurement devices adjacent to the wall. Wells & Worster[18] modeled the wall flows with a two-layer boundary layer structure when the Rayleigh number can reach as large as 10^{20}. The experiment results of Fan *et al.*[19] [20] support the Wells & Worster's theory.
Measurement sites and methods (including modelling of solar radiative heat flux, long wave radiative heat flux and natural convective heat flux) are introduced in chapter 2. Results on ambient conditions, diurnal change of atmosphere transmittance and different type of heat fluxes are gave in chapter 3. Finally, conclusions are summarized in chapter 4.

2. Measurement and methods

The energy balance on the south facing wall surface was calculated based on the energy conservation, which is shown in the Figure 1.

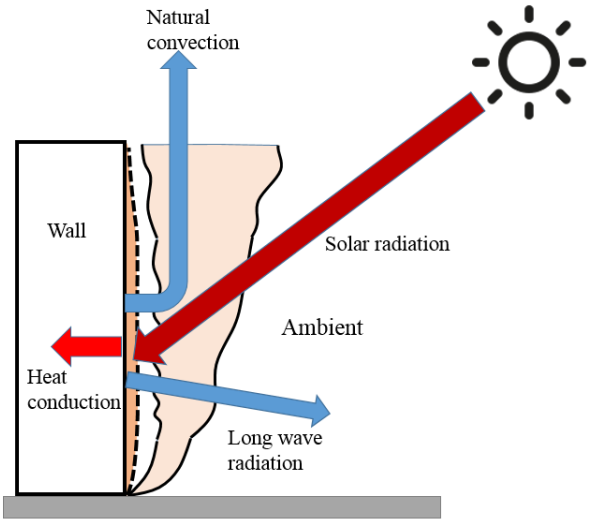

Fig. 1 Heat flux through the wall surface. Heat conduction = Solar radiation - Natural convection - Long wave radiation

The surface temperature were measured by both infrared camera and thermal couples. The uniformity of the wall surface temperature can be shown in Figure 2

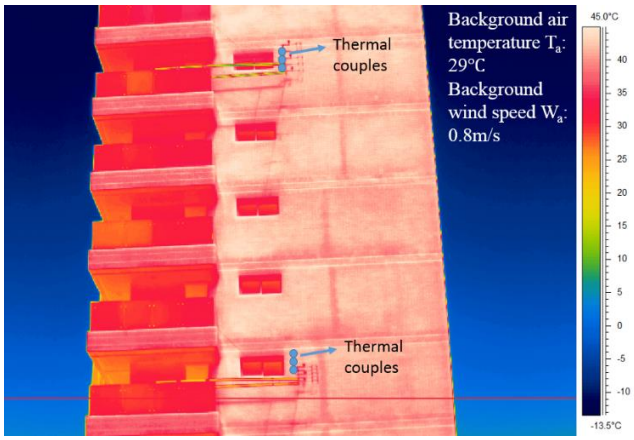

Fig. 2 Infrared picture of the south facing wall. It was taken at 12:00, 15th October. The position of thermal couples are marked on the picture. Only two levels can be observed due to the limitation of the IR camera scope. The two levels shown in the figure is from 10th to 14th floor

2.1. Solar radiation

The position of the sun relative to the horizontal surface can be described by the solar zenith angle θ_z, solar elevation angle α and solar azimuth angle φ, which are illustrated in the Figure 3.

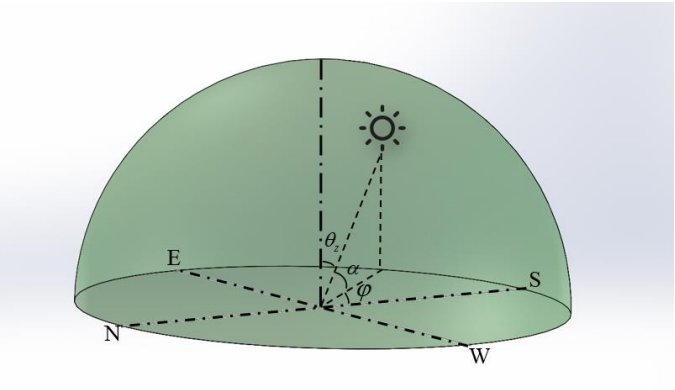

Fig 3. Illustration of solar zenith angle θ_z, solar elevation angle α and solar azimuth angle φ

Solar radiation is the sum of direct solar radiation I_{dir} and diffuse irradiance I_{dif}. The calculation of I_{dir} and I_{dif} are shown in the Equations (1)-(2) given by Bouguer's law:

$$I_{dir} = I_0 E_0 P^{1/\sin\alpha} \cos\theta \tag{1}$$

$$I_{dif} = 0.5 F_{bs} I_0 \sin\alpha \frac{1 - P^{1/\sin\alpha}}{1 - 1.4 \ln P} \tag{2}$$

where I_0 is solar constant with a value of 1367 W m^{-2}, which is recommended by Fröhlich & Brusa [21]; $E_0 = 1 + 0.033\cos(2\pi d_n / 365)$ is defined by Duffie & Beckman [22] as eccentricity correction factor of the earth's orbit and d_n is the day number of the year from 1st January; P is the atmosphere transmittance of solar radiation; α is solar elevation angle (also called solar altitude); θ is solar incidence angle. F_{bs} is shape factor between the calculated surface and sky.
The definition of solar incidence angle is given in Equation (3):

$$\cos\theta = \cos\zeta \cos\theta_z + \sin\zeta \sin\theta_z \cos(\varphi - \gamma) \tag{3}$$

where ζ is the slope of the calculated surface (ζ = 0 when the surface is horizontal and ζ = 90° when the surface is vertical); θ_z is solar zenith angle; φ is solar azimuth angle; γ is the azimuth angle of the calculated surface (γ = 0 when the surface is facing south, γ = 90° when the surface is facing east and γ = -90° when the surface is facing west).
The solar zenith angle θ_z, solar altitude α and solar azimuth φ (φ = 0 when the sun is in south, φ = 90° when the sun is in east and φ = -90° when the surface is in west) are obtained in Equations (4)-(6):

$$\cos\theta_z = \cos\delta \cos\phi \cosh + \sin\delta \sin\phi \tag{4}$$

$$\alpha = 90 - \theta_z \tag{5}$$

$$cos\,\varphi = \frac{sin\,\alpha\,sin\,\phi - sin\,\delta}{cos\,\alpha\,cos\,\phi} \tag{6}$$

where $\delta = 23.45\,sin\left(360 \times \left(d_n + 284\right)/365\right)$ is solar declination; ϕ is the geographic latitude in degrees (the North Hemisphere is positive and the South Hemisphere is negative); $h = 15 \times \left(12 - h_r\right)$ is hour angle (h_r is the local time value, e.g. h_r =12 at noon and h_r =18 at 6 o'clock afternoon).
All the variables to calculate the solar radiation are known except for *P*, the atmosphere transmittance of solar radiation. Fortunately, the solar radiation on the horizontal surface was measured by weather stations, so the transmittance can be calculated by the following Equation (7):

$$I_{measure} = I_{dir} + I_{dif} = I_0 E_0 P^{1/\,sin\alpha}\,cos\,\theta + 0.5 F_{bs} I_0\,sin\,\alpha\,\frac{1 - P^{1/\,sin\alpha}}{1 - 1.4\,ln\,P} \tag{7}$$

The latitude of the measurement point is N 23°06'15''. The experiment was carried out in 14th October to 16th October, 2014. The weather station was set on the roof of the 16 story building and the surrounding area is relatively open, so the shape factor F_{bs} can be assumed to be 1 for the weather station location.
After the transmittance is solved, the short wave radiation on the south facing vertical wall I_{sv} can be calculated by Equation (8):

$$I_{sv} = \left(1 - a\right)\left(I_{dirv} + I_{difv}\right) \tag{8}$$

where *a* is albedo. I_{dirv} and I_{difv} are direct radiation and diffuse radiation on the south facing vertical wall respectively.

2.2. Long wave radiation

The long wave radiation can be divided into two parts: (1) between the vertical wall and sky; (2) between the vertical wall and other ground surfaces. To calculate the long wave radiation between the vertical wall and sky, the sky temperature need to be modeled. Berdahl & Martin (1984)'s sky temperature model has been widely used, which is shown in the Equation (9):

$$T_{sky} = T_a\left[0.711 + 0.0056 T_{dp} + 0.000073 T_{dp}^2 + 0.013\,cos\left(15t\right)\right]^{1/4} \tag{9}$$

where T_{sky} (K) is sky temperature; T_a (K) is ambient dry bulb temperature; T_{dp} (℃) is dew point temperature; *t* is hour from midnight.
The long wave radiation I_{lw} of the vertical wall can be calculated based on Stefan-Boltzmann law by the Equations (10)-(12):

$$I_{lw} = I_{lbs} + I_{lbg} \tag{10}$$

$$I_{lbs} = \sigma \varepsilon_b F_{bs} \left(T_{sky}^4 - T_b^4 \right) \tag{11}$$

$$I_{lbg} = \sigma \varepsilon_b \varepsilon_g F_{bg} \left(T_g^4 - T_b^4 \right) \tag{12}$$

where $\sigma = 5.67 \times 10^{-8}$ W m^{-2} K^{-4} is Stefan-Boltzmann constant. ε_b and ε_g are emissivity for the test building wall surface and surrounding ground respectively. The emissivity of the surrounding surfaces are assumed to be uniform. I_{lbs} is long wave radiation heat flux between the vertical wall and sky. I_{lbg} is long wave radiation between the vertical wall and other surfaces, which is calculated based on simplified equation for non-enclosed envelope. The tested building is much higher than its surroundings and locate in an open area, so the shape factors F_{bs} (shape factor between the building vertical wall and sky) and F_{bg} (shape factor between the building vertical wall and the ground) are assumed to be 0.5. T_b and T_g are surface temperature of the vertical wall and the surface temperature of surround surfaces respectively.

2.3. Natural convective heat transfer

The local convective heat transfer rate can be represented by the non-dimensional Nusselt number Nu_x, which is defined in the Equation (13):

$$Nu_x = \frac{h_x x}{\lambda} \tag{13}$$

where h_x is local convective heat transfer coefficient; x is characteristic length scale, which is vertical coordinate along the wall in this experiment; λ is thermal conductivity.
The local Rayleigh number Ra_x is defined as Equation (14):

$$Ra_x = \frac{g\beta \Delta T x^3}{\nu \kappa} \tag{14}$$

where x is length scale. g is acceleration of gravity. β is thermal expansion coefficient. ΔT is difference between the fluid temperature and ambient temperature. ν is kinematic viscosity. κ is thermal diffusivity.
The correlation between Nu_x and Ra_x for convection is shown in Equation (15):

$$Nu_x = cRa_x^b \tag{15}$$

where c and b are constants. The background wind speed was small when the experiment was carried out. The weather was clear and there was no clouds. The convective heat transfer was dominated by natural convection, which is also confirmed in Fan *et al.* [19] and Fan *et al.* [20]. Therefore, the natural convection correlation between Nu_x and Ra_x can be adopted. Wells & Worster [18] and Fan *et al.* [19] suggested that the flow was in region II, where the buoyancy instability dominate and the heat flux is constant, under this experiment condition. Tsuji &

Nagano [16] and Wells & Worster [18] supported the correlation of natural convection along a heated vertical wall in region II, which is shown as Equation (16):

$$Nu_x = 0.12Ra_x^{1/3} \tag{16}$$

Based on Equations (13)-(16), the heat flux q_x caused by natural convective heat transfer can be obtained as Equation (17):

$$q_x = -h_x \Delta T = -0.12\lambda\left(\frac{g\beta}{\nu\kappa}\right)^{1/3}\Delta T^{4/3} \tag{17}$$

As we can see in the Equation (17), the local heat flux is independent of vertical coordinate x, which means that the heat flux is constant over the wall. Negative in the Equation (17) means the heat flux is from the wall to the ambient air.

2.4. Turbulent flow visualization method by infrared videos

The thermal image method has been adopted by many researchers, such as, Hetsroni, Rozenblit & Yarin [23], Hetsroni & Rozenblit [24], Kowalewski *et al.* [25], Hetsroni *et al.* [26]. Reference[27] gave a detailed description on how to get velocity of the turbulent flow from thermal videos and called the method as thermal image velocimetry (TIV). The general procedure for TIV is shown in Figure 4.

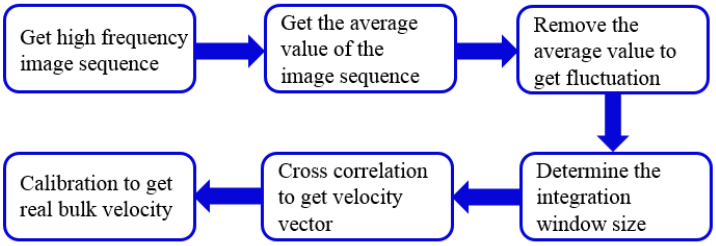

Fig. 4 General procedure of Thermal Image Velocimetry (TIV)

The application of TIV method can be affected by the following factors: (1) the characteristics of tested surfaces (surfaces that have small thermal storage and thermal conductivity are preferred); (2) the temperature difference between the surface and ambient fluid (the temperature difference should be large enough); (3) the resolution of infrared camera; (4) the distance between the camera and the surface (the small distance is preferred. If the distance is large, the infrared ray emitted by the surface can be partially absorbed by the atmosphere between the surface and thermal camera, which will cover the fluctuation of the surface temperature).
Due to the limitations of experiment conditions, such as large thermal storage of the wall, the long distance between the wall and the camera, only qualitative visualization was done.

3. Results

The solar radiation on the building roof is measured by the weather station. The measured solar radiation, calculated diffuse radiation, direct radiation and transmittance are shown in Figure 5.

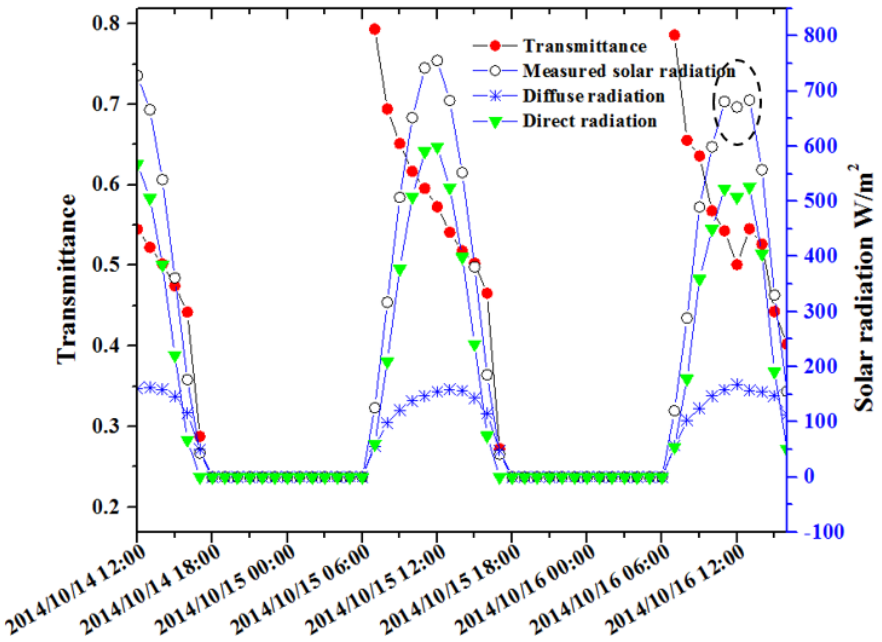

Fig. 5 Solar radiation on the horizontal surface. The transmittance in the figure is atmospheric transmittance of solar radiation

According to Idso [28], the atmospheric transmittance is mainly influenced by three factors: the absorption and scattering by water vapor; the absorption and scattering by dust in the air; scattering by dry dust-free air. The transmittance calculated based on the measured solar radiation keeps decreasing from the sunrise to the sunset.
The diffuse solar radiative heat flux is larger than that of the direct radiation after 16:00 in each day, when the solar elevation angle and transmittance are very small. The direct radiation, diffuse radiation and transmittance have a big fluctuation around 12:00, 16th October (circled by dashed elliptical in Figure 5). The fluctuation is caused by the clouds cover over the sky at that time. The cover of the clouds also show the influence on the ratio of the diffuse radiation to the direct radiation during that period.
The flow along the wall caused by natural convection is shown in Figure 6.

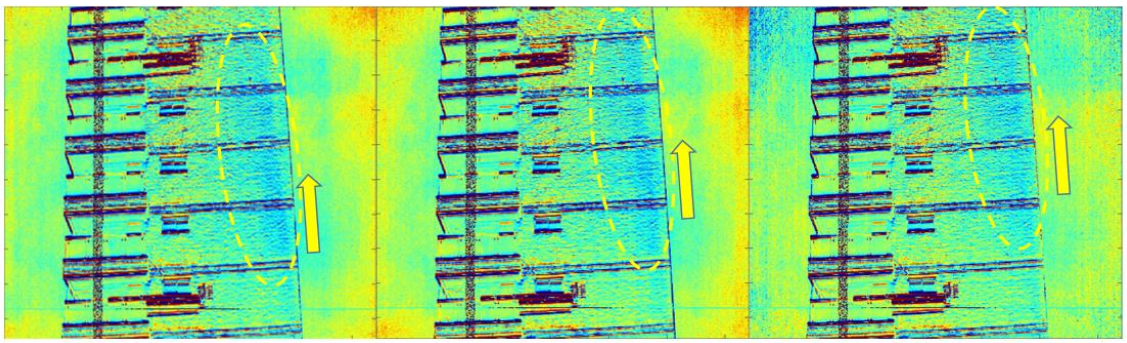

Fig. 6 Visualization of the wall flow caused by natural convection. The average data is obtained from 5 minute image sequence. The temperature shown in the figure is fluctuation after the average is removed. The frequency of videos are 30 Hz. The time interval between (a) (b) and (c) is 1.33 second

The coherent structure circulated by the yellow dashed elliptical in Figure 6 can be observed obviously moving upwardly.
The short wave radiation received by the south facing vertical wall, the heat flux given off by the wall and the conductive heat flux are summarized in Figure 7.

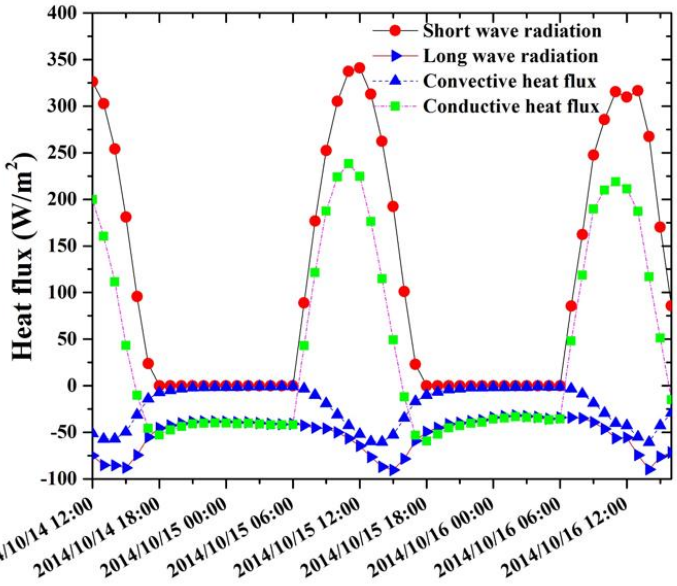

Fig. 7 Energy balance on the wall surface during clear days. The short wave radiation is the received solar radiative heat flux (include direct radiation and diffuse radiation) of the south facing wall. The long wave radiation is the long wave radiative heat flux (include the radiation between the wall and the ground and the radiation between the wall and the sky). The conductive heat flux is the heat conducted into the wall (positive heat flux) and the heat conducted out of the wall (negative heat flux)

As observed in the Figure 7, the phase for different kind of heat fluxes are different under clear day condition. The conductive heat flux into the wall first reach its maximum at around 11:00, and then the short wave radiation appear the peak at around 12:00. The following is the convective heat flux caused by natural convection, when the surface temperature is largest at around 14:00. The long wave radiation heat flux appear its peak in the last at around 15:00. During night time, the heat in the wall is mainly transferred out by long wave radiation. The conductive heat flux out of the wall equal to the long wave radiation heat flux at night. Therefore, if the building density in urban area is too large, it could reduce the long wave radiation and trap the heat in the urban canopy layer. The heat flux caused by natural convection and long wave radiation are in the same order during daytime. The slope of conductive heat flux is large in the morning due to the small slope of convective heat flux and long wave radiation heat flux. The large thermal inertia prevent the wall surface temperature increasing rapidly, leading to the small slope of convective heat flux and long wave radiative heat flux in the morning.

4. Conclusions

The wall flows, surface temperature and radiation along a high-rise building are measured and calculated. The flow along the wall caused by natural convection is visualized by the fluctuation of the surface temperature obtained from the infrared image. The flows along the wall are dominated by natural convection during the calm clear days, so the natural convective heat transfer is used in the energy balance analysis. Solar radiative heat flux

and long wave radiative heat flux are also calculated to complete energy balance model on the wall surface. The atmosphere transmittance is not a constant and keeps decreasing from sunrise to sunset during clear days. The reason is complicated since it can be influenced by the pollutants and water vapor in the atmosphere. The different kind of heat flux reach its maximum value in a day cycle at different time. The conductive heat flux first reach the peak. Afterwards, the solar radiative heat flux get the maximum point and then followed by the natural convective heat flux and long wave radiative heat flux. Natural convective heat flux has the same order with long wave radiative heat flux during day time. Since the heat conduction outside of the wall is dominated by the long wave radiation, the dense high rise buildings will trap the heat in the urban canopy layer.

References:

[1] Barlow JF, Harman IN, Belcher SE (2004) Scalar fluxes from urban street canyons. Part I: Laboratory simulation. *Bound-lay Meteorol*, vol. 113, pp 369-85.
[2] Rotach M, Gryning S-E, Batchvarova E, Christen A, Vogt R (2004) Pollutant dispersion close to an urban surface–the BUBBLE tracer experiment. *Meteorol Atmos Phys*, vol. 87, pp 39-56.
[3] Hang J, Sandberg M, Li Y (2009) Age of air and air exchange efficiency in idealized city models. *Build Environ*, vol. 44, pp 1714-23.
[4] Yang L, Li Y (2009) City ventilation of Hong Kong at no-wind conditions. *Atmos Environ*, vol. 43, pp 3111-21.
[5] Hang J, Li Y (2012) Macroscopic simulations of turbulent flows through high-rise building arrays using a porous turbulence model. *Build Environ*, vol. 49, pp 41-54.
[6] Hernandez M, Medina M, Schruben D (2003) Verification of an energy balance approach to estimate indoor wall heat fluxes using transfer functions and simplified solar heat gain calculations. *Math Comput Model*, vol. 37, pp 235-43.
[7] Ghiaus C (2013) Causality issue in the heat balance method for calculating the design heating and cooling load. *Energy*, vol. 50, pp 292-301.
[8] Naveros I, Bacher P, Ruiz D, Jiménez M, Madsen H (2014) Setting up and validating a complex model for a simple homogeneous wall. *Energ Buildings*, vol. 70, pp 303-17.
[9] Macdonald RW (2000) Modelling the mean velocity profile in the urban canopy layer. vol., pp.
[10] Belcher SE, Jerram N, Hunt JCR (2003) Adjustment of a turbulent boundary layer to a canopy of roughness elements. *J Fluid Mech*, vol. 488, pp 369-98.
[11] Coceal O, Belcher SE (2004) A canopy model of mean winds through urban areas. *Q J Roy Meteor Soc*, vol. 130, pp 1349-72.
[12] Di Sabatino S, Solazzo E, Paradisi P, Britter R (2007) A Simple Model for Spatially-averaged Wind Profiles Within and Above an Urban Canopy. *Bound-lay Meteorol*, vol. 127, pp 131-51.
[13] Eckert E, Jackson TW. Analysis of turbulent free-convection boundary layer on flat plate. 2207: Lewis Flight Propulsion Laboratory Cleveland, Ohio; 1950.
[14] Ostrach S. An analysis of laminar free-convection flow and heat transfer about a flat plate parallel to the direction of the generating body force: National Advisory Committee for Aeronautics; 1952.
[15] Cheesewright R (1968) Turbulent natural convection from a vertical plane surface. *Journal of Heat Transfer*, vol. 90, pp 1-6.
[16] Tsuji T, Nagano Y (1988) Turbulence measurements in a natural convection boundary layer along a vertical flat plate. *Int J Heat Mass Tran*, vol. 31, pp 2101-11.
[17] Abu-Mulaweh H, Chen T, Armaly B (2000) Effects of free-stream velocity on turbulent natural-convection flow along a vertical plate. *Exp Heat Transfer*, vol. 13, pp 183-95.
[18] Wells AJ, Worster M (2008) A geophysical-scale model of vertical natural convection boundary layers. *J Fluid Mech*, vol. 609, pp 111-37.
[19] Fan Y, Li Y, Hang J, Wang K (2015) Wall flows along a high-rise building. *Unpublished Manuscript*, vol., pp.

[20] Fan Y, Li Y, Hang J, Wang K (2015) Estimate the flow rate caused by high-rise building walls natural convection in urban canopy layer. *Unpublished Manuscript*, vol., pp.
[21] Fröhlich C, Brusa R. Solar radiation and its variation in time. Physics of Solar Variations: Springer; 1981. p. 209-15.
[22] Duffie JA, Beckman WA. Solar engineering of thermal processes: Wiley New York etc.; 1980.
[23] Hetsroni G, Rozenblit R, Yarin L (1996) A hot-foil infrared technique for studying the temperature field of a wall. *Measurement Science and Technology*, vol. 7, pp 1418.
[24] Hetsroni G, Rozenblit R (2000) Thermal patterns on a heated wall in vertical air–water flow. *Int J Multiphas Flow*, vol. 26, pp 147-67.
[25] Kowalewski T, Mosyak A, Hetsroni G (2003) Tracking of coherent thermal structures on a heated wall. *Exp Fluids*, vol. 34, pp 390-6.
[26] Hetsroni G, Kowalewski T, Hu B, Mosyak A (F2001) Tracking of coherent thermal structures on a heated wall by means of infrared thermography. *Exp Fluids*, vol. 30, pp 286-94.
[27] Inagaki A, Kanda M, Onomura S, Kumemura H (2013) Thermal image velocimetry. *Bound-lay Meteorol*, vol. 149, pp 1-18.
[28] Idso SB (1969) Atmospheric attenuation of solar radiation. *J Atmos Sci*, vol. 26, pp 1088-95.